

Doping induced metal-insulator phase transition in NiO

S. Sharma,* J. K. Dewhurst, and E. K. U. Gross

1 Max-Planck-Institut für Mikrostrukturphysik, Weinberg 2, D-06120 Halle, Germany.

(Dated: March 7, 2013)

The insulator to metal phase transition in NiO is studied within the framework of reduced density matrix functional theory and density functional theory. We find that the spectral density obtained using reduced density matrix functional theory is in good agreement with experiments both undoped as well as doped NiO. We find that the physical description of the hole-doping induced phase transition *qualitatively differs* depending on whether NiO is calculated within density functional theory or reduced density matrix functional. In the former case the underlying mechanism of the phase transition is identified to be a rigid shift of chemical potential, while in the latter case a redistribution of the spectral weight drives the transition. These latter results are found to be in good agreement with both experiments and previous many-body calculations.

PACS numbers:

The antiferromagnetic Mott insulators present one of the outstanding challenges to the first principles treatment of extended solids. The prototypical example of such a system is NiO, an antiferromagnetic Mott insulator with a measured gap of 4.1eV and a magnetic moment of $1.7 \mu_B$. The standard local density approximation (LDA) within density functional theory (DFT) predicts a metallic spectrum for NiO, in fundamental disagreement with experimental reality. The inclusion of spin polarization via the local spin density approximation (LSDA) results in a small gap, and a description of NiO as a Slater insulator. However, both the gap and the magnetic moment are severely underestimated suggesting that the Slater antiferromagnetic state obtained within the LSDA does not describe the true nature of NiO.

In order to overcome this deficiency of the LSDA Kohn-Sham (KS) spectra, Rödl *et al.* proposed the use of two separate fitting parameters: an on-site Coulomb term U and a scissors shift Δ , where Δ is the difference between the experimental gap and the KS gap obtained using LSDA+ U functional[1]. With a certain choice of these two parameters the KS spectra of NiO can be made to agree with computationally expensive many-body techniques such as dynamical mean field theory (DMFT)[2–5], reduced density matrix functional theory (RDMFT)[6], and the G_0W_0 method[1]. This scissors corrected LSDA+ U method comes under the heading of the so called correlated band theory method.

What makes NiO even more interesting is its behavior as a function of doping: one finds a insulator metal phase transition (IMT) on doping the system with Li, which amounts to hole doping[7]. The physics of this phase transition found to be very rich due to a subtle interplay of charge transfer and Mott localization: despite being a text book Mott insulator, NiO also has a strong charge transfer character due to the large overlap (in energy) of the Ni d and O- p states. Any theory attempting to capture this IMT in NiO must be capable of treating

Mott correlations and charge transfer effects on an equal footing, presenting a significant theoretical challenge.

In the present work we study the IMT in NiO using three different approaches: the local spin density approximation (LSDA) within DFT, correlated band theory method, LSDA+ U , and a many-body technique, RDMFT. In doing so we demonstrate that even though at zero doping all these methods give similar spectra, the physics of hole doping phase transition is *qualitatively different* for the different theoretical methods: within band and correlated band theory methods the metalization occurs due to rigid shifting of the chemical potential into the valence band, with the separation between the Hubbard bands remaining approximately constant. In total contrast to this, within RDMFT one finds that the phase transition is driven by a transfer in spectral weight from the upper and lower Hubbard bands to a low energy peak, known as the correlated peak. These latter results we find to be in excellent agreement with previous many-body results obtained using DMFT[5].

Recently, RDMFT has shown potential for correctly treating band as well as Mott insulators[6, 8, 9], or in other words, treating both Mott correlations and charge transfer effects on an equal footing. Within RDMFT, the one-body reduced density matrix (1-RDM) is the basic variable [10, 11]

$$\gamma(\mathbf{r}, \mathbf{r}') \equiv N \int d^3r_2 \dots d^3r_N \Psi(\mathbf{r}, \mathbf{r}_2 \dots \mathbf{r}_N) \Psi^*(\mathbf{r}', \mathbf{r}_2 \dots \mathbf{r}_N), \quad (1)$$

where Ψ denotes the many-body wave function and N is the total number of electrons. Diagonalization of γ produces a set of orthonormal Bloch functions, the so called natural orbitals[10], $\varphi_{i\mathbf{k}}$, and occupation numbers, $n_{i\mathbf{k}}$. Extending RDMFT to the truly non-collinear magnetic case[6], by treating the natural orbitals as two component Pauli-spinors, leads to the spectral representation

$$\gamma(\mathbf{r}, \mathbf{r}') = \sum_{i\mathbf{k}} n_{i\mathbf{k}} \varphi_{i\mathbf{k}}(\mathbf{r}) \otimes \varphi_{i\mathbf{k}}^*(\mathbf{r}'). \quad (2)$$

The necessary and sufficient conditions for ensemble N -representability of γ were provided, in a classic work, by Coleman[12]. These conditions require

$$\begin{aligned} 0 &\leq n_{i\mathbf{k}} \leq 1 \\ \sum_{i\mathbf{k}} n_{i\mathbf{k}} &= N. \end{aligned} \quad (3)$$

In terms of γ , the total ground-state energy [11] of the interacting system is (atomic units are used throughout)

$$\begin{aligned} E[\gamma] &= -\frac{1}{2} \text{tr}_\sigma \int \lim_{\mathbf{r} \rightarrow \mathbf{r}'} \nabla_{\mathbf{r}}^2 \gamma(\mathbf{r}, \mathbf{r}') d^3 r' + \int \rho(\mathbf{r}) V_{\text{ext}}(\mathbf{r}) d^3 r \\ &+ \frac{1}{2} \int \frac{\rho(\mathbf{r}) \rho(\mathbf{r}')}{|\mathbf{r} - \mathbf{r}'|} d^3 r d^3 r' + E_{\text{xc}}[\gamma], \end{aligned} \quad (4)$$

where $\rho(\mathbf{r}) = \text{tr}_\sigma \gamma(\mathbf{r}, \mathbf{r})$, V_{ext} is a given external potential, and E_{xc} we call the exchange-correlation (xc) energy functional. In principle, Gilbert's [11] generalization of the Hohenberg-Kohn theorem to the 1-RDM guarantees the existence of a functional $E[\gamma]$ whose minimum, for fixed a V_{ext} , yields the exact γ and the exact ground-state energy. In practice, however, the correlation energy is an unknown functional of γ and needs to be approximated. While there are several known approximations for the xc energy functional, the most promising for extended systems is the power functional[8] where the xc energy is given by

$$E_{\text{xc}}[\gamma] = -\frac{1}{2} \int \int d^3 r' d^3 r \frac{|\gamma^\alpha(\mathbf{r}, \mathbf{r}')|^2}{|\mathbf{r} - \mathbf{r}'|} \quad (5)$$

with α indicating the power in the operator sense. In view of the universality of the functional $E_{\text{xc}}[\gamma]$, the value of α should, in principle, be system-independent. A few "optimum values" of α have been suggested in the literature[8, 13, 14]; in the present work α is fixed to 0.656.

In order to the study the doping dependent metalization of NiO one crucially needs spectral information. To obtain this information from RDMFT, which by its very nature is a ground-state theory, is a difficult task. In this work we extract spectral density from RDMFT using the method recently proposed in Ref. [6]. Within this method the diagonal of the spectral density, the so called density of states, is determined using the following relation:

$$\text{DOS} = 2\pi \sum_{\lambda} [n_{i\mathbf{k}} \delta(\omega - \epsilon_{i\mathbf{k}}^-) + (1 - n_{i\mathbf{k}}) \delta(\omega + \epsilon_{i\mathbf{k}}^+)] \quad (6)$$

where

$$\epsilon_{i\mathbf{k}}^\pm = \left. \frac{\partial E[\{\phi\}, \{n\}]}{\partial n_{i\mathbf{k}}} \right|_{n_{i\mathbf{k}}=1/2}. \quad (7)$$

This method is known to produce accurate spectra for finite systems[15] as well as solids[6]. Following the above procedure the spectral density for doped and undoped NiO is calculated using the full-potential linearized augmented plane wave [16] code Elk[17].

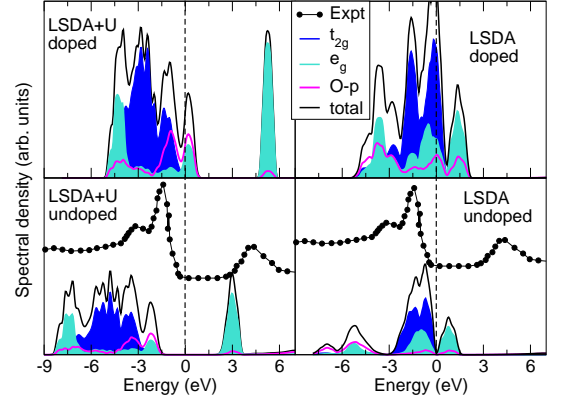


FIG. 1: (Color online) Projected and total density of states for NiO as a function of energy (in eV). Results are shown for undoped (lower panels) and hole doped (upper panels) NiO. The results are obtained using two different functionals within DFT; the LSDA (left panels) and the LSDA+ U method (right panels). Experimental data from Ref 18 is also presented for comparison.

We first examine the behaviour of undoped NiO within band and correlated band theory by using LSDA and LSDA+ U methods; results for total DOS and the site and symmetry projected spectral density are presented in Fig. (1). One can observe that while the LSDA band gap is grossly underestimated as compared to experiment, a *rigid shift* of the valence band to lower energies would result in a spectrum with an overall shape in good agreement with experiment. Indeed, the correct ordering of the t_{2g} and e_g states is obtained within LSDA, i.e., the band gap, even though underestimated, separates a t_{2g} valence and a e_g conduction band, with a substantial overlap of e_g and t_{2g} states in the valence band.

On applying an on-site Coulomb repulsion the the gap opens, but at the cost of a deterioration in the agreement of the overall spectral weight with experiment. In particular, the band ordering is now found to be incorrect at precisely the value of U that leads to the correct

	Undoped	Doped
LSDA		
Ni- t_{2g}	5.42	4.81
Ni- e_g	2.43	2.43
O- p	1.73	1.51
LSDA+ U		
Ni- t_{2g}	5.52	5.52
Ni- e_g	2.19	1.80
O- p	1.78	1.51
RDMFT		
Ni- t_{2g}	5.49	5.49
Ni- e_g	2.27	2.27
O- p	1.88	1.08

TABLE I: Number of electrons in various site and symmetry projected states. Results obtained for undoped and hole doped (with 1.2 holes per formula unit) NiO obtained using the LSDA, the LSDA+ U method, and RDMFT.

magnitude of the gap, which occurs between purely e_g states. This striking defect of the LSDA+ U treatment of NiO was also noticed in Ref. 1, and the use of a smaller U with an additional external parameter, the so called scissors correction Δ , was suggested as a remedy. However, while the spectrum of the equilibrium ground state is improved by this procedure, albeit with the use of an additional fitting parameter, such an approach cannot be used to study the insulator to metal transition in NiO: the very meaning of the parameter Δ is lost once the material enters the metallic phase.

Upon doping the KS spectrum shows a rather simple behaviour for both LSDA and LSDA+ U methods; the chemical potential rigidly moves into the valence band leading in consequence to metalization. We may estimate the distribution of the added hole by integrating the site and symmetry projected DOS up to the chemical potential. The values of the electronic charge in various symmetry states are presented in Table I. It is clear that in total contrast to the experimental situation [7], within the LSDA and LSDA+ U methods the added holes are equally distributed between the Ni d and O p -states.

We now consider the situation where NiO is treated within RDMFT, see Fig. (2). Firstly, it is obvious that the total spectral density obtained for undoped NiO is in good agreement with experiments[18]. The spectrum at high energies (12-15eV), which within DMFT is somewhat broadened due to analytic continuation, is brought out very clearly by RDMFT. The value of the band-gap obtained using RDMFT (4.88eV) is larger than experiments (4.1eV), and the magnetic moment ($1.38\mu_B$) smaller than the experimental value of $1.7\mu_B$. There are two reasons for the smaller value of the magnetic moment within RDMFT as compared to experiment. Firstly, the calculations are performed with the FP-LAPW method

in which space is divided into spheres around the atoms, the so called muffin-tins, and an interstitial region. In the case of fully non-collinear magnetic calculations the magnetic moment per site is calculated by integrating the magnetization vector field inside the muffin-tin. This implies the loss of a small part of the moment to the interstitial region. Secondly, the power functional induces a slight non-collinearity in the magnetization leading to yet more loss in the integrated z -projected moment.

The site and symmetry projected spectral density is also shown in Fig. (2). In good agreement with previous many-body studies[19, 20], we find that the conduction band is purely e_g in character. A substantial overlap of Ni d and Oxygen p states may be seen in the valence spectrum, highlighting the presence of charge transfer effects in NiO.

Turning to the hole doping of NiO, we find that the effect on the spectral density is strikingly different within RDMFT, as compared to both the LSDA and LSDA+ U methods. Hole doping is found to lead to a redistribution of spectral weight from the upper and the lower Hubbard bands towards the chemical potential, which in turn leads to an IMT. If one uses the correlated band theory definition of U as being roughly equal to the distance between the upper Hubbard band and the correlated peak, then it is evident that the value of U changes as a function of doping. An additional striking difference between DFT and RDMFT results is that the added hole is mostly localized in the O p -states (the precise amount of charge in various orbitals is presented in Table I), in marked contrast to the equal distribution between Ni d - and O p -states found within LSDA and LSDA+ U method. These results are in excellent agreement with experiments in which it is observed that the added holes have mainly O- p character.

As shown in Fig. 2, the spectral density of doped NiO is also in good agreement with available experimental data[7]. Turning to the quantitative description of the phase transition afforded by RDMFT, we find that the substantial metalization occurs at a somewhat higher value of hole doping than observed in experiments (0.5 holes). There are two principle reasons for this. Firstly, the undoped gap for NiO (4.88eV) is larger than the experimental value, and hence additional hole doping with be required to drive the material to the metallic state. Secondly, we do not study the effect of an actual impurity added to the system but rather the hole doping is simulated, as in previous works, by the removal of electronic charge from the unit cell while adding a constant compensating positive background to ensure charge neutrality. This method is commonly known as the virtual crystal approximation. Interestingly, previous DMFT calculations also identified the transfer in spectral weight as the driving mechanism for the hole doping transition in NiO[5], and many of the features identified in this article were also found in the DMFT treatment of NiO. We

thus find that RMDFT treatment of NiO is much close to many-body theories such as the DMFT, than to the LSDA or correlated band approaches.

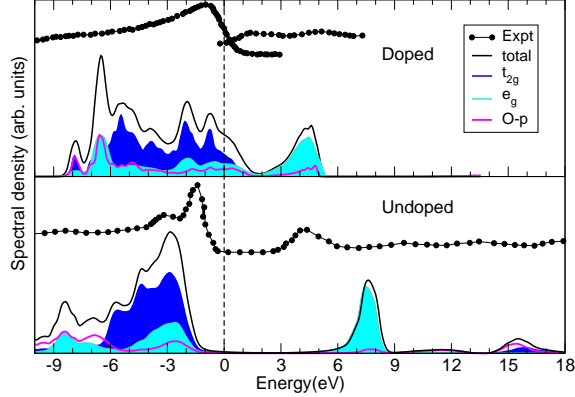


FIG. 2: (Color online) Total and projected spectral density for NiO, obtained using RDMFT, as a function of energy (in eV). Results are presented for undoped (lower panel), hole doped with 1.2 holes per formula unit (upper panel). Experimental results from Ref. 18 and 7 are presented for comparison.

To summarize we have presented the physics behind the doping induced insulator to metal phase transition in NiO and have found that the physics of phase transition is brought out in strikingly different ways by different theoretical methods: within DFT based studies metalization occurs due to a rigid shifting of the chemical potential into the valence band, with the separation between the Hubbard bands remaining approximately constant. In contrast, within RDFMT the phase transition is driven by a transfer in spectral weight from the upper and lower Hubbard bands to what is known as the correlated peak. The RDMFT results closely resemble those of the dy-

namical mean field theory.

* Electronic address: sharma@mpi-halle.mpg.de

- [1] C. Rödl, F. Fuchs, J. Furthmüller, and F. Bechstedt, Phys. Rev. B **79**, 235114 (2009).
- [2] W. Metzner and D. Vollhardt, Phys. Rev. Lett. **62**, 324 (1989).
- [3] A. Georges, G. Kotliar, W. Krauth, and M. J. Rozenberg, Phys. Rev. B **68**, 13 (1996).
- [4] J. Kunes, A. V. Lukoyanov, V. I. Anisimov, R. T. Scalettar, and W. E. Pickett, Nat. Mat. **7**, 198 (2008).
- [5] J. Kunes, V. I. anisimov, A. V. Lukoyanov, and D. Vollhardt, Phys. Rev. B **75**, 165115 (2007).
- [6] S. Sharma, S. Shallcross, J. K. Dewhurst, and E. K. U. Gross, <http://www.arxiv.org>, cond-mat: arXiv:0912.1118 (2009).
- [7] J. V. Elp, H. Eskes, P. Kuiper, and G. A. Sawatzky, Phys. Rev. B **45**, 1612 (1992).
- [8] S. Sharma, J. K. Dewhurst, N. N. Lathiotakis, and E. K. U. Gross, Phys. Rev. B **78**, 201103 (2008).
- [9] N. N. Lathiotakis, S. Sharma, N. Helbig, J. K. Dewhurst, M. A. L. Marques, F. Eich, T. Baldisiefen, A. Zacarias, and E. K. U. Gross, Zeitschrift für Physikalische Chemie **224**, 467 (2010).
- [10] P. O. Lödwin, Phys. Rev. **97**, 1974 (1955).
- [11] T. L. Gilbert, Phys. Rev. B **12**, 2111 (1975).
- [12] A. Coleman, Rev. Mod. Phys. **35**, 668 (1963).
- [13] N. Lathiotakis, S. Sharma, J. Dewhurst, F. Eich, M. Marques, and E. Gross, Phys. Rev. A **79**, 040501 (2009).
- [14] A. Putaja and E. Rasanen, Phys. Rev. B **84**, 035104 (2011).
- [15] E. N. Zarkadoula, S. Sharma, J. K. Dewhurst, E. K. U. Gross, and N. N. Lathiotakis, Phys. Rev. A **85**, 032504 (2012).
- [16] D. J. Singh, Planewaves Pseudopotentials and the LAPW Method, Kluwer Academic Publishers, Boston (1994).
- [17] (2004), URL <http://elk.sourceforge.net>.
- [18] G. A. Sawatzky and j. W. Allen, Phys. Rev. Lett. **53**, 2339 (1984).
- [19] X. Ren, I. Leonov, G. Keller, M. Kollar, I. Nekrasov, and D. Vollhardt, Phys. Rev. B **74**, 195114 (2006).
- [20] A. Fujimori, F. Minami, and S. Sugano, Phys. Rev. B **29**, 5225 (1984).